Korea Polymer Journal, Vol. 9, No. 4, pp 228-237 (2001)

The Evolution of Rigid Amorphous Fraction and Its Correlation with the Glass Transition Behavior in Semicrystalline Bisphenol-A Polycarbonate

Seungman Sohn

Department of Chemistry and Materials Science and Engineering, Virginia Polytechnic Institute and State University, Blacksburg, VA 24061, USA

Received June 18, 2001

Abstract : The evolution of conformational constraints in bisphenol-A polycarbonate (BAPC) upon quiescent bulk crystallization was quantitatively analyzed from calorimetric study employing a rigid amorphous fraction (RAF) as an indicator of the level of conformational constraints. From the correlation between corrected crystallinity (X_c) and total rigid fraction (f_r), it was found that, regardless of molar mass distribution and thermal treatment conditions, semicrystalline BAPC always exhibits greater f_r than X_c maintaining a quantitative relationship of $f_r \approx 2X_c$ in the range of $0.0 < X_c < 0.4$. This directly indicates the evolution of approximately the same amount of RAF as X_c (i.e., RAF$\approx X_c$) upon bulk crystallization of BAPC. It was also found that T_g *per se* and T_g broadening enhance as RAF increases, and there appears to be a critical level of RAF (>0.2) needed to initiate significant changes in both quantities.

Introduction

Historically the morphology of semicrystalline polymers has been envisaged through a simple two-phase model namely "fringed-micelle" model, in which tacitly only two clear-cut phases are assumed: crystalline and amorphous phases.[1] This fringed micelle model has been applied in a limited basis to describe the morphology and the structure-property relationship of rubber, cellulose, and polymers with low crystallinity.[2] For example, in the explanation of observed increase of the strength in an elastomer with crystallinity, this model suggests that the pinning effect of embedded crystalline phase will increase the strength; therefore, as crystallinity increases modulus enhances as well.

In reality, however, the existence of interphase between crystalline and unconstrained amorphous regions often challenges the simplicity of the two-phase model. Two intrinsic restrictions in polymer crystallization- chain entanglement in amorphous phase due to the long chain nature of polymers and higher folding energy in basal plane (σ_e) compared with the lateral plane (σ_s)- are at the origin of creating an interphase. Largely speaking but certainly with exceptions, σ_e is in the range of 40 to 100 mJ/m^2, and σ_s is in the vicinity of 5 to 20 mJ/m^2. This relatively large surface free energy in chain folding plane often gives rise to a considerable penalty limiting the thickness of polymer lamellar crystals as well as depressing the apparent melting temperature. Furthermore, various types of imperfections such as non-adjacent chain folds, tie molecules and chain cilia may also contribute to form an interphase between lamellar crystals and disordered free melt.

Numerous experimental observations suggest the existence of interphase. These are 1) in calorimetric study, the lower intensity of relaxation strength at T_g (ΔC_p at T_g) was observed even after considering the effect of crystallinity, e.g., poly (oxymethylene) (POM),[4] polyethylene (PE),[5] isotactic polypropylene (it-PP),[6] poly(caprolactone),[7] isotactic polystyrene (it-PS),[8] poly(butylene terephthalate) (PBT),[9] poly(ethylene terephthalate)

*e-mail : seungman@lgchem.co.kr

(PET),[7,10] poly(phenylene sulfide) (PPS),[11,12] poly (ether ether ketone) (PEEK),[13] and thermoplastic polyimide (TPI)[14]; 2) in dielectric measurement, the unexpected decrease of α-relaxation intensity in the presence of crystals was proposed as an evidence of the existing interphase, e.g., TPI,[14] PEEK[15]; 3) in dynamic mechanical analysis, the broadening and shifting of T_g in semicrystalline polymers was often detected, e.g., TPI,[16] bisphenol-A polycarbonate (BAPC)[17]; 4) in SAXS study, direct measurement of the interphase thickness was made in a few polymers, e.g., PPS,[11] TPI.[14] All of these diverse and independent techniques unanimously agree on the existence of the interphase, although some of fundamental questions regarding its physical nature remain still open.

Among various examples indicating the existence of interphase, the lower relaxation strength in semicrystalline polymers at glass transition has long been known. In principle, *the change in heat capacity at T_g (ΔC_p at T_g) must reveal the relaxation strength of all the amorphous chains undergoing glass transition.* Therefore, the intensity of ΔC_p step or the relaxation strength at T_g for semicrystalline polymers will be diminished because the fraction of amorphous chains participating in glass transition has been reduced. Under a strict application of the two-phase model, heat capacity change at T_g can be used to determine the crystallinity of a given semicrystalline system through a simple relationship, if ΔC_p associated with the amorphous state is known:

$$X_c = 1 - f_{maf} = 1 - \Delta C_p^{sc}/\Delta C_p^{am} \quad (1)$$

Where X_c is crystallinity, f_{maf} is a fraction of mobile amorphous phase, and ΔC_p^{sc} and ΔC_p^{am} are the heat capacity changes at T_g in the semicrystalline and completely amorphous polymers, respectively. Eq. (1) assumes that all the amorphous polymer chains relax at T_g and that polymer chains in the crystalline phase do not.

In fact, many authors, including Wunderlich *et al.*[4,6,7,9,10,12,13] and Cebe *et al.*[11,14] observed that the right side of Eq. (1) is greater than the crystallinity measured either from calorimetry or from other independent techniques such as WAXS. These results strongly suggest that in the case of semicrystalline polymers, especially in rigid backbone polymers, *not all the amorphous chains relax at the normal glass transition temperature.* Based on this observation, Wunderlich *et al.* introduced the concept of *rigid amorphous fraction* (RAF), which is, in definition, the fraction of amorphous chains that does not relax at the normal glass transition temperature.[6,18,19] Accordingly, Eq. (1) may be reformulated as follows.

$$f_r = 1 - \Delta C_p^{sc}/\Delta C_p^{am} \quad (2)$$

$$f_r = X_c + f_{raf} \quad (3)$$

Where f_r is a total rigid fraction, the summation of crystallinity (X_c) and rigid amorphous fraction (f_{raf}).

Later on, Cebe *et al.* further developed this concept to explain some of structure-property relationships of semicrystalline polymers. They reported several interesting observations from the study of PPS such as the increase of RAF with decreasing molar mass, the increase of RAF with decreasing (melt or cold) crystallization temperature, and appearance/disappearance of RAF depending on the crystallization and annealing conditions.[11,14] More importantly they observed the glass transition temperature was qualitatively related to the degree of RAF.[11,14]

Despite these studies, more complete picture, such as the effects of molar mass distribution and thermal treatments on the level of RAF, has not been emerged. This is particularly important in that chemical and/or physical properties of semicrystalline polymers will be affected by the conditions of crystallization and subsequent thermal treatment, and these changes may, at least qualitatively, be associated with the development of conformational constraints. Often the conformational constraints exerted by semicrystalline polymers can be visualized as the increase of T_g or T_g broadening:[11,14,20] whereas in some cases, conformational constraints assumed to be related to the level of RAF[11,14] developed in due course of various thermal treatments. In this regard, the aims of present work were directed first to show a clear development of RAF upon various thermal treatments, and second to find a correlation of T_g or T_g broadening with

RAF. Hopefully these observations may further our understanding of the development of conformational constraints in semicrystalline polymers. Similar to previous communications,[21-23] BAPC was used as a model system exploiting its extremely slow crystallization kinetics to study the effects of time, temperature, and molar mass on its development of conformational constraints.

At this moment a caution needs to be taken in that the level of crystallinity must be determined as accurately as possible for a proper evaluation of RAF (see Eq. (2) and (3)). In many cases, the crystallinity is expressed as the ratio of a certain measured quantity in semicrystalline polymer to that in 100% crystalline phase. For instance, crystallinity from calorimetry is often expressed as follows.

$$X_c = \Delta H_m^{exp}/\Delta H_m^{o} \quad (4)$$

where ΔH_m^{exp} and ΔH_m^{o} are the experimental and 100% crystalline phase heat of fusion, respectively. At least two corrections need to be considered for a proper use of Eq. (4). First, ΔH_m^{o} represents the enthalpy of fusion of a perfect crystal at *the equilibrium melting temperature*, T_m^{o}. However, semicrystalline polymers usually melt at a lower temperature than T_m^{o}; thus, ΔH_m^{exp} needs to be corrected for a temperature effect. Second, ΔH_m^{o} assumes the infinitely large perfect crystal, yet in reality, polymer crystals are limited in size, thus the surface enthalpic contribution should be taken into account. In this paper the crystallinity of all the data presented was properly corrected considering above two effects, and based on this more accurate crystallinity and RAF were evaluated.

Experimental

Materials Preparation and Characterization. Bisphenol-A polycarbonate (BAPC) samples investigated in the present work are commercial grades manufactured by General Electrics under the trade name of "Lexan" and some of near monodisperse fractions, obtained through a solvent/non-solvent fractionation starting from one of the commercial sample. The details of the fractionation process have been published elsewhere.[23] Molecular characteristics of these materials were determined by means of GPC (solvent: HPLC grade chloroform) using standard PS and BAPC samples. Therefore, the molar masses reported here are absolute values. For each sample, measurement was repeated for three times, and the reproducibility was better than ±10%. Weight average molar masses and the polydispersity indices (M_w/M_n) of the samples are listed in Table I, where the fractions are marked by asterisk. Commercial samples were provided to us in the form of pellets, and were further purified by dissolving in chloroform followed by precipitation with methanol. It was subsequently washed several times with clean methanol and then dried in the oven at 150 °C for a period of 24 hrs to remove any possible solvent traces. In order to avoid the degradation of BAPC due to water absorption, all samples were dried in a vacuum oven above the T_g of the polymer for 24 hrs and kept dry throughout the experiments. Amorphous films of 120±20 μm thickness were prepared by compression molding of the dry samples at 250 °C/150 psi under a nitrogen atmosphere for 5 minutes. Sample was subsequently cooled down to room temperature. These films were transparent, and were further shown to be amorphous from density measurements.

Crystallization and Thermal Treatments.

Bulk Crystallization: Amorphous films thus prepared were then wrapped with Kapton® film inside and aluminum foil outside, and were crystallized in an oven under an inert atmosphere. Oven temperature scale was calibrated and temperature control was better than ± 0.3 °C. All the samples were crystallized at T_c for the time of t_c from the glassy state, yet crystallization conditions, as indicated in Table I, were slightly varied among samples to induce a similar temperature difference between T_c and T_g of each sample.[24] Thus prepared samples were further reshaped for various thermal treatments and calorimetry measurements.

Isothermal Secondary Crystallization: Bulk crystallized samples were partially melted at T_{pm}, and further exposed to isothermal secondary crystallization (ISC) experiments at various T_x for different times. ISC experiments were conducted inside a DSC for a better temperature control

Table I. Molecular Characteristics, Crystallization and Subsequent Thermal Treatment Conditions for Commercial and Fractionated BAPC. PM and ISC Represent, Respectively, Partial Melting and Isothermal Secondary Crystallization

Sample	M_w (g·mol^{-1})	M_w/M_n	Initial Crystallization Conditions		PM T_{pm} (°C)	ISC T_x (°C)
			T_c (°C)	t_c (hrs)		
*PC-4K	4,270	1.02	165	38	216	-
*PC-6K	6,110	1.05	173	49	215	163 - 178
*PC-12K	12,400	1.10	178	160	220	168 - 183
*PC-17K	17,100	1.10	181	382	-	-
PC-19K	18,800	1.99	170	384	217	-
PC-28K	28,400	2.00	185	202	220	165 - 195

Asterisk denotes fractions.

(±0.1 °C). Partial melting (PM) was performed to clearly resolve the temporal evolution of low endotherm from the multiple melting behavior of original sample. In the previous reports, it was shown that PM did not affect the most probable populations of main lamellae, and thus the variation of RAF upon overall crystallization and ISC could be independently pursued.[21-23] ISC was performed at three different T_xs of below, at, and slightly above T_c.

Crystallization temperature (T_c), time (t_c) and partial melting temperature (T_{pm}) are listed in Table I.

The Effect of Cooling Rate: To investigate the effect of cooling rate on the evolution of conformational constraints, PC-28K samples, bulk crystallized at 185 °C for 202 hrs and partially melted at 220 °C, were exposed to cooling experiments from T_{pm} to 100 °C (i.e., *ca.* 45 °C below T_g). Various cooling rates in the range of 0.32 °C/min to 40 °C/min were employed. Results including thermograms were reported elsewhere.[21]

Isothermal Annealing: In contrast to ISC experiments, during which the main lamellar morphology did not change, isothermal annealing (IA) performed well above T_c was found to significantly increase the apparent melting temperature in the DSC suggesting an isothermal lamellar thickening.[22] In other words, we can control the main lamellar structure by IA. To further our understanding of the effect of main lamellar morphology change on the development of conformational constraints, high temperature isothermal annealing experiments were conducted well above T_c. For this, fully crystallized PC-28K samples were annealed at five different temperatures (T_a = 208, 214, 217, 220, 223 °C) for various times in the range of 1 minute to 20 hrs. Upon reaching the desired annealing time, sample was fast cooled to 100 °C, and heating traces were recorded. For all these different stages of sample preparation, crystallization and annealing, GPC results confirmed that the molar mass and molar mass distribution of the samples have not been modified.

Calorimetric Measurements.

Differential Scanning Calorimetry: Differential scanning calorimetry (DSC) was used for the monitoring of thermal behavior in amorphous or semicrystalline BAPC. A DSC-2 Perkin-Elmer calorimeter operated with an ice and water bath was used. Heating traces were recorded at 10 °C/min unless otherwise specified. In order to reduce differences among samples, discoid samples of 120± 20 mm thickness and 11.0± 1.0 mg weight were employed. A linear horizontal baseline of the DSC signal was obtained before and after a few series of DSC scans. This baseline corrects for the difference between the heat flow output of a blank DSC pan and the reference pan to zero or a constant. The heat flow output for the sample was obtained after subtraction of the baseline heat flow from the recorded output for that sample. In the ΔC_p measurement, sapphire calibration was done for each sample and scan rate. Temperature

calibration during cooling scans was achieved by recording the isotropic-to-nematic phase transition of *p*-azoxyanisole. The known temperature for the reversible isotropic to nematic phase transition of this liquid crystal is equal to 136.0°C. Temperature calibration during heating scans was accomplished by recording the melting transition of an indium standard sandwiched between two amorphous BAPC films.[21] This step was necessary for a correct temperature calibration in the experiments with different heating rates, since polymers have lower thermal conductivity than metal standards.

Evaluation of Heat Capacity Change: Heat capacity change (ΔC_p) at T_g and the broadness of T_g have been measured following the method of Cheng *et al.*[13] As illustrated in Figure 1, T_g was determined at the inflection point of the ΔC_p increase. T_g broadening (ΔT_g) was measured by the temperature difference in the intercepts of the tangential line at T_g with the heat capacity lines of liquid (T_2) and glass (T_1) (i.e., $\Delta T_g = T_2 - T_1$). In the present work, over 180 DSC melting traces, in which each thermogram represents sample with different thermal history such as crystallization and subsequent thermal treatments, were carefully analyzed. In each heat flow, rigid fraction, f_r, and the experimental heat of fusion (ΔH_m^{exp}) were determined. Thus obtained ΔH_m^{exp} was properly corrected to evaluate an accurate crystallinity considering the two aforementioned factors: 1) temperature correction for the experimental heat of fusion (for details, see Appendix), and 2) surface enthalpic contribution for the equilibrium heat of fusion.[25] Finally, RAF for each DSC curve was determined from the difference between rigid fraction and corrected crystallinity.

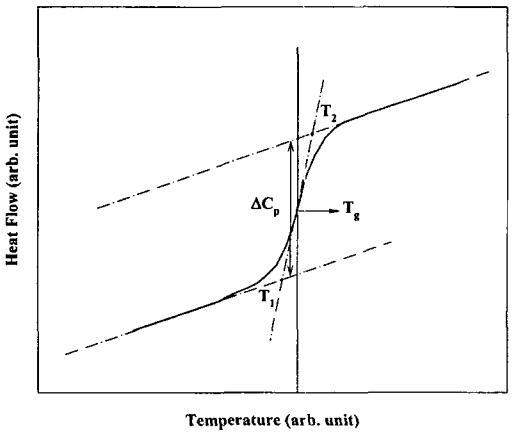

Figure 1. A schematic DSC traces in the glass transition region.

Results

Amorphous Characterization. After fractionation and purification, amorphous samples were characterized in terms of glass transition temperature (T_g) and heat capacity change at T_g (ΔC_p at T_g). This step is an important precursor to crystallization study since amorphous state can serve as a "zero" crystallinity state. Glass transition temperatures and heat capacity changes are, respectively,

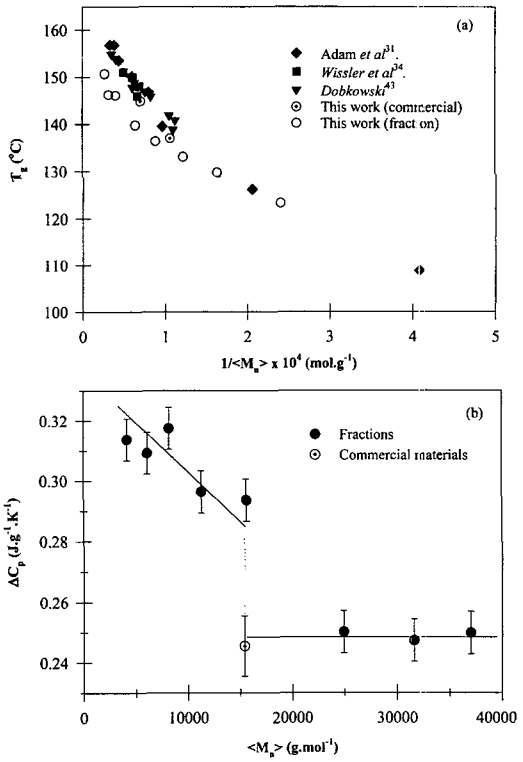

Figure 2. (a) Variation of amorphous BAPC glass transition temperature as a function of $<M_n>^{-1}$. The polydispersity of fractions used in the present study was in the range of 1.02 to 1.49 and polydispersity for literature data including the commercials in this work is in the range of 2.0 to 3.5; (b) Heat capacity change at T_g (ΔC_p at T_g) as a function of number average molar mass of amorphous BAPC.

presented in Figure 2(a) and 2(b), in which literature data have been included for comparison. Since glass transition temperature is sensitive to the method employed, literature data[11-14] obtained from calorimetry under similar conditions (HR = 10 °C/min) are only included.

Figure 2(a) clearly shows the increase of T_g with molar mass. The variation of T_g is over 25 °C for the number average molar mass ranging between *ca.* 4,200 and 37,000 g mol^{-1}. The particular way of presenting T_g shown in this figure follows the Fox-Flory equation,[26] in which the variation of T_g has been empirically approximated as a linear function of $<M_n>^{-1}$. Overall, the agreement between the data from this study and from the literature is acceptable, with the exception of somewhat lower T_gs of high molar mass fractions from this study. Similar results have been reported from the study of polystyrene. Monodisperse and polydisperse samples of polystyrene are indistinguishable when their glass transition temperature is expressed as a function of M_n.[27]

In Figure 2(b), the variation of ΔC_p (HR = 10 °C/min) of amorphous BAPC as a function of molar mass is shown. The main feature is that with a decrease of molar mass, ΔC_p at T_g increases. Similar results have been reported for other polymers.[28] Of more interest, above a certain molar mass (≈15,000 g/mol), ΔC_p seems to be constant being equal to 0.25 $J \cdot g^{-1} \cdot K^{-1}$. In regards to ΔC_p of BAPC of similar range of molar mass between 25,000 to 45,000 $g \cdot mol^{-1}$, several studies[28-34] reported the value being in the range of 0.17 to 0.3 $J \cdot g^{-1} \cdot K^{-1}$, in which the most frequent value[29,30,32-34] is close to 0.24 $J \cdot g^{-1} \cdot K^{-1}$. The average value of 0.25 $J \cdot g^{-1} \cdot K^{-1}$ from this study agrees with the results from the previous reports. These ΔC_ps at T_gs for amorphous samples were used to evaluate the quantitative level of total rigid fraction in Eq. (2).

Analysis of Calorimetric Data. Before presenting the DSC analysis results, we need to specify the sample nomenclature used in the following figures. All the samples were designated as (PC-XX, t_c, YY, T_x). PC-XX stands for the molar mass of PC samples; t_x, for the time of primary crystallization; YY, for the method of thermal treatment; and T_x, for the temperature of ISC. YY could be ISC (isothermal secondary crystallization), IA(isothermal annealing), BC(bulk crystallization), and CL(cooling). For example (PC-28K, t_x = 153 hrs, ISC, 185 °C) means PC-28K sample initially crystallized at 185 °C for 153 hrs, partially melted at 220 °C, and subsequently exposed to ISC at 165 °C for various times (see Table I for T_{pm} and T_c).

In Figure 3, the evolution of rigid fraction (f_r) as a function of corrected crystallinity is presented. One immediate observation is that regardless of molar mass and various thermal treatment conditions, all the data fall on the same line within the limit of experimental uncertainty. More importantly, f_r is always greater than X_c, being approximately, f_r

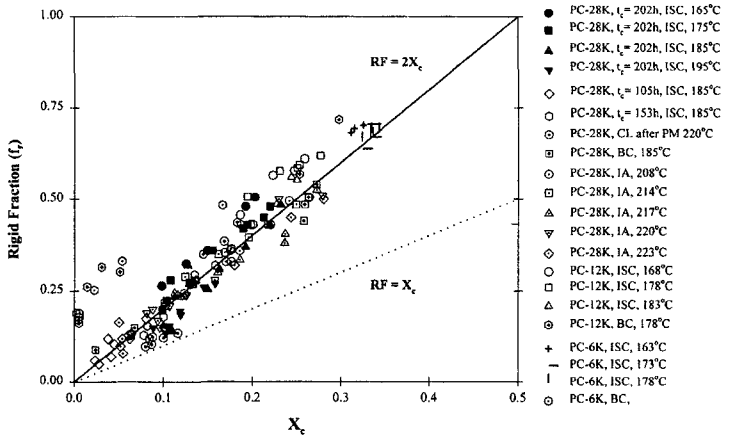

Figure 3. The evolution of rigid fraction (f_r) as a function of crystallinity for BAPC samples thermally treated under various conditions. Note that crystallinity has been temperature corrected.

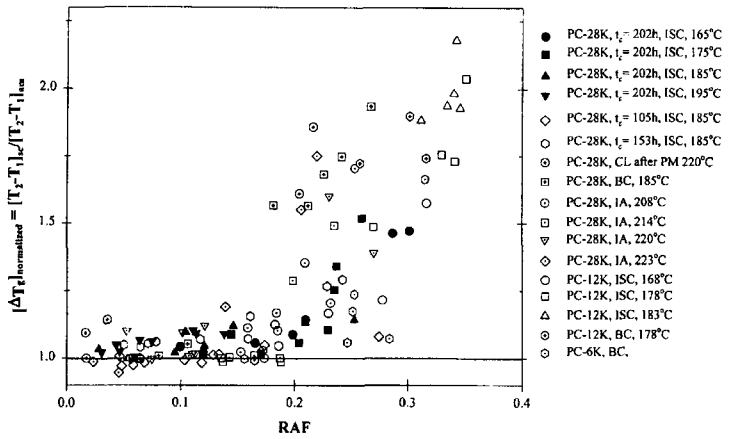

Figure 4. T_g broadening as a function of RAF in BAPC samples under various thermal Treatments.

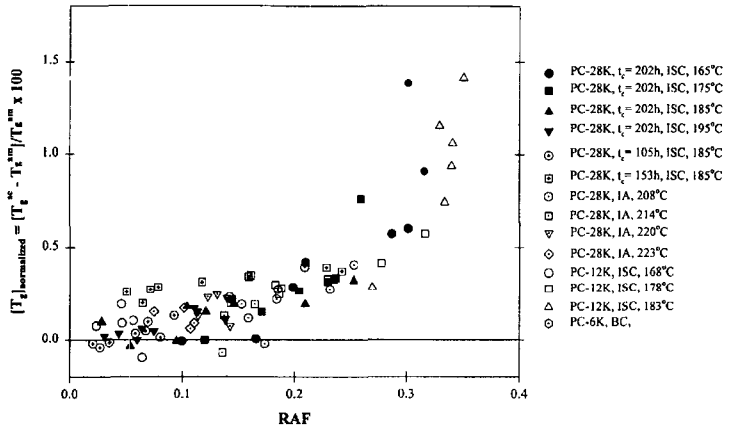

Figure 5. Normalized T_g increase as a function of RAF for BAPC samples under various thermal treatments.

$\approx 2X_c$ in the range of $0.0 < X_c < 0.4$. According to Eq. (3), this result indicates that *RAF increases almost linearly with crystallinity*; furthermore, RAF becomes negligible when crystallinity approaches zero value. The dotted line inserted in Figure 3 denotes the predicted relationship if a two-phase model holds for the morphology of this system. Despite of relatively large scattering of measurements, it can be clearly stated that the application of a two-phase model is an oversimplification in the case of semicrystalline BAPC. Another interesting observation is that lower molar mass samples, crystallized either from BC or ISC, exhibit higher level of RAF compared with higher molar mass samples.

In Figure 4 and 5, respectively, normalized T_g broadening and T_g variation as a function of RAF are shown. $[\Delta T_g]_{normalized}$ was defined as $[T_2\text{-}T_1]_{sc}/[T_2\text{-}T_1]_{am}$, in which *sc* and *am* stand for semicrystalline and amorphous phase. T_g variation was also normalized in a similar way as $[T_{g,\,normalized} = [T_g^{sc} - T_g^{am}]/T_g^{am} \times 100$. Largely speaking, these two plots show a similar trend: an increase of RAF leads to the increase of T_g and T_g broadening regardless of molar mass and distribution, and conditions of various thermal treatments.

Discussion

As seen in Figure 3, the inequality between f_r and X_c is a clear deviation from the two-phase model. In the context of this model, f_r should be

the same as X_c, because amorphous (mobile) and crystalline (rigid) phases are only assumed. Within experimental uncertainty, the observation of $f_r \approx 2X_c$ may suggest the upper limit of apparent maximum crystallinity achievable from the bulk crystallization of BAPC. This is because, hypothetically, when f_r reaches 1, the corresponding crystallinity would be 0.5. Obviously, f_r can not be greater than 1; therefore, $X_c = 0.5$ would be the upper boundary of crystallinity observable in BAPC bulk crystallization. It is well known that when BAPC (M_w = ca. 25,000 to 67,000 g $\cdot$mol^{-1}) is crystallized from the bulk, the kinetics of crystallization are extremely slow and the maximum degree of crystallinity seldom exceeds 0.3.[17,34-39] In the present study, even from the isothermal annealing experiments (see the data labeled as IA in Figure 3), the maximum crystallinity did not exceed 0.28, being the highest value among all of the PC-28K samples crystallized under various conditions. Further, in the cases of lower molar mass fractions, even though the rate of primary crystallization kinetics was increased more than 100 times compared with that of PC-28K,[23,40] surprisingly, the final level of crystallinity was always less than 0.37. In general, these slow crystallization kinetics and limited crystallizability of BAPC have been explained in terms of chain rigidity.[37,41,42] The above observation in Figure 3 may suggest a more specific result of chain rigidity: rigid chains may generate higher level of RAF (i.e., more conformational constraints) and this will further hinder the growth of crystals, which eventually limits the final level of crystallinity.

In Figure 3, it can be also observed that the lower molar mass sample exhibits a higher degree of RAF. Cebe *et al.* reported a similar result from the study of cold-crystallized PPS.[14] They explained the observation in such a way that the lower molar mass sample has a greater number of taut tie molecules between the crystals resulting in a large fraction of constrained amorphous phase.[14] For BAPC, this could be because of the increased crystallinity of low molar mass fractions due to the increased mobility. To strictly compare RAF in various samples differing in molar masses, the crystallinity as well as the method of crystallization should be the same; however, during ISC, the first condition could not be met due to the relatively fast crystallization kinetics and higher degree of crystallinity in lower molar mass fractions.[24,40] Nonetheless, the sets of data for lower molar mass fractions obtained from BC supports the previous observation that molar mass appears to be inversely related to the level of RAF developed during crystallization.[14]

The increase of T_g and T_g broadening with the increase of RAF in Figure 4 and 5 may be expected, if the assumption that the level of RAF is indicative to the development of conformational constraints. This assumption appears, at least qualitatively, to be acceptable, since the level of RAF clearly leads to the increase of T_g broadening as well as T_g per se. Of more interest, however, is that T_g increase or broadening significantly occurs only above a certain level of RAF, seemingly close to the value of 0.2. Because the data are less scattered below this value, this upturn point can be relatively well defined. Based on the assumption that the location of the RAF could be between the lamellar crystals, possibly near the crystal/amorphous interphase, a plausible explanation may be proposed. Before the RAF reaches a certain critical value, the thickness of amorphous layer is large enough not to be affected by the presence of RAF (insignificant change in T_g and T_g broadening). However, as the RAF further increases, more constrained amorphous will show a retarded relaxation leading to the significant increase of T_g and T_g broadening. At this later stage, due to the large scattering of measurements, no other specific information such as the effects of molar mass and thermal treatments could be obtained; however, qualitatively speaking, T_g and T_g broadening increase dramatically at this stage, indicating the existence of considerable conformational constraints.

Conclusions

From the analysis of calorimetric data of varying molar mass BAPC samples crystallized under various conditions, it was found that, regardless of molar mass and thermal treatment conditions, semicrystalline BAPC exhibits a rigid fraction (f_r) that is always greater than the corrected crystallinity (X_c). This observation strongly suggests the

evolution of RAF upon bulk crystallization of BAPC. Quantitatively, the degree of the RAF increases almost linearly with crystallinity in the range of 0 to 0.4, and the lower molar mass samples show a higher degree of RAF compared with higher molar mass samples. T_g and T_g broadening increase with the evolution of RAF, and, of more interest, it seems that there exists a critical level of RAF (>0.2) that initiates the significant changes in T_g and T_g broadening. This unambiguous correlation between RAF and glass transition behavior supports the proposal that, in semicrystalline polymers, conformational constraints developed during crystallization and thermal treatments may be quantitatively evaluated using RAF as an indicator.

Acknowledgements. It is greatly acknowledged for the kind supply of BAPC fractions by Mr. L. C. Shank and Dr. H. D. Iler as well as helpful discussions from Dr. A. Alizadeh.

Appendix

Temperature Correction for the Experimental Heat of Fusion. Temperature correction for the experimental heat of fusion was done using the following thermodynamic considerations. The enthalpy of fusion, ΔH_m^* at a temperature T_m will be given by:

$$H_m^*(T_m) = H_m^0(T_m^0) + \int_{T_m}^{T_m^0} C_p'(T)dT \quad \text{(A1)}$$

$$\Delta C_p'(T) = C_p^L(T) - C_p^S(T) \quad \text{(A2)}$$

Where $\Delta C_p'(T)$ is the difference between the heat capacities of the solid and liquid polymers at temperature T. The temperature dependencies of heat capacities of BAPC in both liquid and glassy states are available experimentally. In addition, Wunderlich *et al.* in the ATHAS databank[44] provided the temperature dependence of the heat capacity of BAPC in the *crystalline state* based on theoretical considerations. In this study, a value of 608K has been used for the equilibrium melting temperature of BAPC.[34] Figure A1 shows a calibration curve used for the temperature correction of the experimental heat of fusion in BAPC crystallized from the bulk. Note that PC-6K (fraction) and PC-28K (commercial), which represent two extreme molar masses used for the analysis, fall on the same line. The experimental heat of fusion in each DSC curve used in the present study has been temperature corrected based on the calibration factor given in Figures A1, and thus obtained value was used for the proper evaluation of crystallinity.

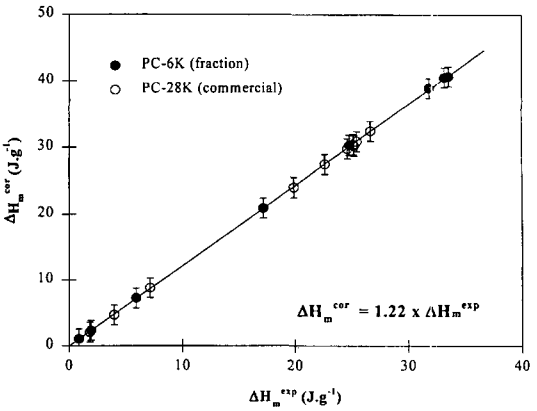

Figure A1. A temperature correction curve for the experimental heat of fusion in BAPC Samples.

References

(1) J. Schultz, *Polymer Materials Science,* Prentice-Hall, Inc, Englewood Cliffs, New Jersey, 1974.
(2) J. H. Magill, *Morphogenesis of Solid Polymer Microstructure,* in *Treaties on Materials Science and Technology, Volume 10, Properties of Solid Polymeric Materials, Part A,* J. M. Schultz, Ed.. Academic Press, New York, 1977.
(3) L. Mandelkern, *The Crystalline State,* in *Physical Properties of Polymers,* J. E. Mark, Ed., ACS Washington D.C, 1984.
(4) H. Suzuki, J. Grebowicz, and B. Wunderlich, *British Polym. J.,* **17**, 11 (1985).
(5) C. L. Beatty and F. E. Karasz, *J. Macromol. Sci.-Rev. Macromol. Chem.,* **C17**, 37 (1979).
(6) J. Grebowicz, S. F. Lau, and B. Wunderlich, *J. Polym. Sci.: Polym. Symp.,* **71**, 19 (1984).
(7) J. Menczel and B. Wunderlich, *J. Polym. Sci. Polym. Lett. Ed.,* **19**, 265 (1981).
(8) F. E. Karasz, H. E. Bair, and J. M. OReilly, *J. Phys. Chem.,* **69**(8), 2657 (1965).
(9) S. Z. D. Cheng, R. Pan, and B. Wunderlich, *Macromol. Chem.,* **189**, 2443 (1988).
(10) B. Wunderlich, *Thermal Analysis,* Academic Press,

Sandiego, CA, 1990.
(11) P. Huo and P. Cebe, *Colloid Polym. Sci.*, **270**, 840 (1992).
(12) S. Z. D. Cheng, Z. Q. Wu, and B. Wunderlich, *Macromolecules*, **20**, 2802 (1987).
(13) S. Z. D. Cheng, M. Y. Cao, and B. Wunderlich, *Macromolecules*, **19**, 1868 (1986).
(14) P. P. Huo, J. B. Friler, and P. Cebe, *Polymer*, **34**, 4387 (1993); S. X. Lu, P. Cebe, and M. Capel, *Macromolecules*, **30**, 6243 (1997).
(15) P. Cebe and P. P. Huo, *Thermochimica Acta*, **238**, 229 (1994).
(16) S. Srinivas and G. L. Wilkes, *Polymer*, **39**, 5839 (1998).
(17) E. Laredo, M. Grimau, A. Muller, A. Bello, and N. Suarez, *J. Polym. Sci. Polym. Phys.*, **34**, 2863 (1996).
(18) S. F. Lau and B. Wunderlich, *J. Polym. Sci. Polym. Phys.*, **22**, 379 (1984).
(19) H. Suzuki, J. Grebowicz, and B. Wunderlich, *Macromol. Chem.*, **186**, 1109 (1985).
(20) H. Marand, A. Alizadeh, R. Farmer, R. Desai, and V. Velikov, *Macromolecules*, **33**, 3392 (2000); H. Marand, A. Alizadeh, R. Farmer, R. Desai, and V. Velikov, *Bull. Am. Phys. Soc.*, **44**(1), 608 (1999).
(21) S. Sohn, A. Alizadeh, and H. Marand, *Polymer*, **41**, 8879 (2000).
(22) S. Sohn, A. Alizadeh, H. Marand, L. C. Shank, and H. D. Iler, *American Chemical Soc. Polym. Preprint*, **81**, 250 (1999).
(23) A. Alizadeh, S. Sohn, H. Marand, L. C. Shank, and H. D. Iler, *Macromolecules*, **34**, 4066 (2001).
(24) In a strict sense, to compare the level of RAF among various samples with different molar masses, T_c for each sample needs to be set to lead to the same undercooling, i.e., $\Delta T = T_m^\circ - T_c$, where T_m° is an equilibrium melting temperature. Unfortunately, at present, the equilibrium melting temperatures of BAPC fractions are not available; thus assuming at least qualitatively the shift of T_g is related to the increase of T_m° of a given polymer, this criterion was applied.
(25) S. Sohn, A. Alizadeh, and H. Marand, manuscript in preparation.
(26) P. J. Flory, *J. Appl. Phys.*, **21**, 581 (1950); *J. Polym. Sci., Part C*, **16**, 3373 (1968).
(27) P. L. Kumler, S. E. Keinath, and R. F. Boyer, *J. Macromol. Sci. Phys.*, **B13**, 631 (1977).
(28) R. F. Boyer, *J. Macromol. Sci. Phys.*, **B7**, 487 (1973).
(29) S. Z. D. Cheng and B. Wunderlich, *J. Polym. Sci. Polym. Phys.*, **24**, 1755 (1986).
(30) B. Wunderlich and L. D. Jones, *J. Macromol. Sci. Phys.*, **B3**, 67 (1969).
(31) G. A. Adam, J. N. Hay, I. W. Parsons, and R. N. Haward, *Polymer*, **17**, 51 (1976).
(32) E. A. DiMarzo and F. Dowell, *J. Appl. Phys.*, **50**, 6061 (1979).
(33) W. Kim and C. M. Burns, *J. Appl. Polym. Sci.*, **34**, 945 (1987).
(34) G. E. Wissler and B. Crist, *J. Polym. Sci. Polym. Phys.*, **18**, 1257 (1980).
(35) J. M. Jonza and R. S. Porter, *J. Polym. Sci. Polym. Phys.*, **24**, 2459 (1986).
(36) E. Turska, W. Przygocki, and M. Maslowski, *J. Polym. Sci. Part C*, **16**, 3373 (1968).
(37) G. Mendez and A. J. Müller, *J. Thermal Analysis*, **50**, 593 (1997).
(38) B. Falkai and W. Rellensmann, *Makromolekular Chem.*, **75**, 112 (1964).
(39) G. V. Di Filippo, M. E. Gonzalez, M. T. Gasiba, and A. V. Müller, *J. Appl. Polym. Sci.*, **34**, 1959 (1987).
(40) S. Sohn, Ph. D dissertation, *The effects of time, temperature, and molar mass on the crystallization behavior of bisphenol-A polycarbonate*, April, 2000, Blacksburg, Virginia, Virginia Polytechnic Institute and State University, USA.
(41) Hermann Schnell, *Chemistry and Physics of Polycarbonates*, John Wiley & Sons, Inc, 1964.
(42) G. Kämpf, *Kolloid-Zeitschrift*, **172**, 50 (1960).
(43) Z. Dobkowski, *Eur. Polymer J.*, **18**, 563 (1982).
(44) ATHAS data Bank: http://funnelweb.utcc.utk.edu/~athas/databank/intro.html.